

## Chapter 2

# Compositional and seismic structure of the mantle

## 2.1 Compositional models

Three classes of compositional models are being used.

### Chondritic

Meteorites, Earth rocks and solar abundances have on average very similar compositions, especially for the non-volatile elements. This composition has been proposed to be representative for the composition in the original solar system. Important differences occur for the more volatile elements, which have been attributed to formation processes. If an average composition based on chondritic (the so-called stony, least differentiated) meteorites is taken as representative for the mantle+core+crust, a mantle composition can be estimated from differentiation models. There are some problems with the chondritic composition however, starting with the Mg/Si ratio (two of the main components of the mantle), which have led to doubts on the homogeneity of the original nebula. Therefore the chondritic model is used nowadays as a general reference that brackets the range in which a reasonable Earth composition should fall, and not so much anymore as a model that provides the detailed composition of the Earth.

### Petrological

Models of melting relations are used to determine the composition of a source rock that (1) generates a basalt when melting and (2) is related to the most primitive mantle rock samples found at the surface such as xenoliths and tectonically emplaced peridotites. This has led to the compositional model called pyrolite (a *pyroxene-olivine* rock), first proposed by Ringwood. Various versions of pyrolite have been proposed. They all more or less have the following composition:

In terms of oxides	(wt %)	In terms of minerals	(vol %)
$SiO_2$	45	olivine ( $Mg_{0.98}, Fe_{0.11}$ ) $_2SiO_4$	57
$MgO$	38	orthopyroxene ( $Mg, Fe$ ) $SiO_3$	17
$FeO$	7.8	clinopyroxene ( $Ca, Mg, Fe$ ) $_2Si_2O_6 - NaAlSi_2O_6$	12
$Al_2O_3$	4.4	pyrope-rich garnet ( $Mg, Fe, Ca$ ) $_3(Al, Cr)_2Si_3O_{12}$	14
$CaO$	3.5		
$Na_2O, Fe_2O_3$	small amounts		

Pyrolite is the most accepted (but not only) model for the composition of at least the upper mantle and it fits the seismic properties of both upper and lower mantle within the uncertainties. The model provides estimates for major as well as minor elements. Pyrolite occurs in different phases as material goes through a series of phase transition when traveling from the surface to the bottom of the mantle.

However, the pyrolite model does not seem to be a good source rock (in its minor elements) for all volcanic products found at the surface, particularly not for those brought up at ocean islands ('hotspots'). Furthermore, important differences with the whole Earth composition estimated from meteorites have fueled an ongoing debate about the validity of the pyrolite model.

### Seismological

Here  $V_P$ ,  $V_S$  and  $\rho$  inferred from seismic data are compared with laboratory and theoretical estimates of the

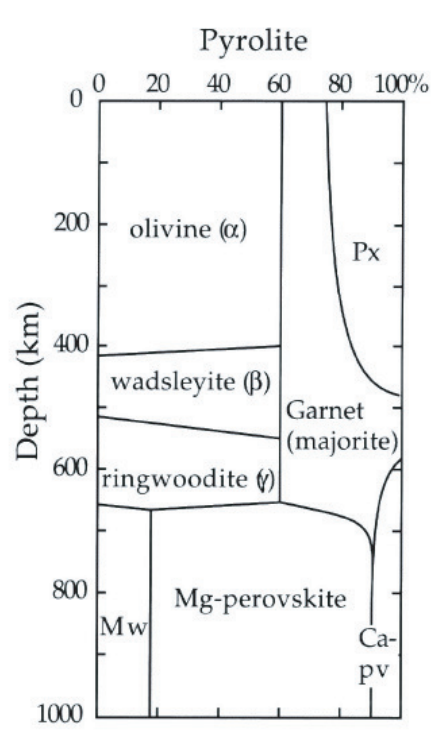


Figure 2.1: Pyrolite in its various phases throughout the mantle

elastic parameters and density for various minerals at mantle pressures and temperatures. This provides estimates on the major element composition of the Earth but does not provide any constraints on the minor components, among which the heat producing elements and many of the tracers used by geochemists.

## 2.2 Compositional constraints from mass and moment of inertia

Using

$$g = \frac{GM}{a^2} \quad (2.1)$$

with gravitational acceleration  $g = 9.8 \text{ m/s}^2$ , the gravitational constant  $G = 6.67 \times 10^{-11} \text{ Nm}^2\text{kg}^{-2}$  and the Earth's radius  $a = 6371 \text{ km}$ , gives the total mass of the Earth  $M = 5.974 \times 10^{24} \text{ kg}$ . This implies that the average density of the Earth is  $5.5 \times 10^3 \text{ kg/m}^3$ , which is significantly higher than the density of  $2.5 - 3.3 \times 10^3 \text{ kg/m}^3$  of surface rocks.

The angular momentum for the Earth  $I \approx 0.33Ma^2$  is less than  $I = 0.4Ma^2$  which would be expected for a homogeneous sphere, implying that mass is more concentrated towards the center of the Earth. For a spherically symmetric Earth:

$$M = 4\pi \int_0^a \rho(r')r'^2 dr' \quad (2.2)$$

$$I = \frac{8\pi}{3} \int_0^a \rho(r')r'^4 dr' \quad (2.3)$$

With estimates of the depth of the core mantle boundary from seismology the first estimates of the average density of the mantle and core were made: using the above 2 equations in a 2-layer Earth (mantle+core) with the core radius  $a_{CMB} = 0.5a_{Earth}$  leads to a system of two equations with two unknowns, which is easily solved. It suggests an average mantle density  $\rho_m = 4600 \text{ kg/m}^3$  and an average core density  $\rho_c = 14000 \text{ kg/m}^3$ . These values suggest that the average mantle density is higher than what we observe near the surface, and that the core is too dense to be rocky, and needs to be a metal, most probably iron based on the chondritic and solar abundances of different elements.

## 2.3 Adiabatic compression

What causes the increase in density with depth? Is it simply the self-compression, the increase with density as a result of the increasing pressure with depth? This can be tested by calculating the change in density due to adiabatic compression and comparing the resulting density profile with seismological constraints and the total mass and moment of inertia for the Earth. From the definition of compressibility it follows that:

$$\left[ \frac{\partial \rho}{\partial P} \right]_S = \frac{\rho}{K_S} \quad (2.4)$$

Thus:

$$\left[ \frac{\partial \rho}{\partial r} \right]_S = \left[ \frac{\partial \rho}{\partial P} \right]_S \frac{dP}{dr} = \frac{\rho}{K_S} \cdot (-\rho g) = -\frac{\rho g}{\phi} \quad (2.5)$$

The last equation is called the Adams-Williamson equation, and describes the change in density purely due to adiabatic self-compression. From a seismic profile of bulk sound velocity the equation can be integrated to give density as a function of depth. Adams and Williamson did this (in 1923) starting with a surface mantle density of 3 and  $3.5 \times 10^3 \text{ kg/m}^3$ . They found that the average Earth density obtained in this manner is significantly less than the observed average density, leading to the conclusion that there has to be a change in composition with depth. A layer that does fit the adiabatic density increase is nowadays called an Adams-Williamson layer, or shortly a A-W layer.

Bullen (1942) repeated this exercise, but after dividing the Earth in various layers, and tested whether adiabatic self-compression is a valid assumption for the upper and lower mantle and outer and inner core, using a different starting density for each layer. He found that he could find a reasonable starting density (consistent with surface rocks for the mantle, and iron for the core) for the upper 400 km, the lower mantle and the core, but not for the transition zone from about 400 to about 1000 km depth. He already proposed this could be due to the occurrence of phase transitions in this depth range. But even today the debate as to whether the stronger increase in density in the transition zone is only due to phase transitions or a change in chemistry also occurs continues.

## 2.4 Birch's law

Seismic velocity measurements have been used since long to constrain the Earth's composition. A significant step forward in the seismic constraints on this composition of the Earth came with the introduction of Birch's law. Birch's law is an experimental relation between  $V_P$ , specific mass  $\rho$  and mean atomic mass  $\bar{M}$  (the sum of all atomic masses divided by the number of atoms). Most of the close-packed mantle oxides and silicates have a value of  $\bar{M}$  close to 20. An increase in iron content increases  $\bar{M}$ .  $\bar{M}_{mantle} = 21.1$ ,  $\bar{M}_{core} = 49.3$ . Birch fit a linear law to laboratory  $V_P - \rho$  data:

$$V_P = a(\bar{M}) + b\rho \quad (2.6)$$

Compositions proposed for the mantle (pyrolite with its high-pressure assemblages) lie along a  $\bar{M}$  is constant line. Any density and  $V_P$  estimates for the core clearly show that it must have a much higher mean atomic mass than the mantle, and this mass can be compared with the mean atomic mass for compositions measured in the laboratory, i.e., under low P,T conditions. This confirms that the core must mainly consist of iron, with the addition of a few percent of a lighter element to the outer core.

## 2.5 1-D seismic velocity structure

Much of the information on the internal structure of the mantle is derived from seismology. Other geophysical data, such as gravity, orbital parameters, and electromagnetic data provide constraints on the integrated structure of the Earth, but little about the depth and lateral variations.

The various seismic wave types (body waves, surface waves and free oscillations) each provide different information on the Earth's internal structure. Analyses done early last century already provided important constraints on the 1-D structure. They documented a velocity increase at about 30 km depth (crust-mantle boundary - Mohorovicic in 1909) and at 410 and 660 km depth, and a strong velocity decrease at about 2900 km depth (core-mantle boundary - Oldham in 1906, Gutenberg in 1914). Furthermore it was found that no S waves appear to pass through the core, which led to the conclusion that the core must liquid. A bit later (Lehmann in 1936) it was found that the core actually consists of an inner and outer core, and normal mode data showed that the inner

core must be solid, something that was only very recently (2000) confirmed with the observation of inner core S waves. One-dimensional seismic velocity models based on travel time, surface wave and normal mode data, such as the model PREM (Preliminary Reference Earth Model, [Dziewonski and Anderson(1981)]) fit the observations within 5-10%. Thus to a very good first approximation the Earth has a spherically symmetric structure.

Starting with the first 1-D seismic velocities models these models have been used to constrain the thermal and compositional structure of the Earth, in combination with gravity data and orbital parameters that provide the total mass, total angular momentum and radius of the Earth, as described above.

Normal mode data as included in the derivation of the PREM model are not only sensitive to seismic velocities but also to density. The constraints on density are however not as strong as the constraints that the combination of body waves, surface waves and normal modes provides for velocity structure. To constrain densities in PREM it was required that the total mass and angular moment agree with those observed, that the lower mantle, outer and inner core are as close as the data allow to A-W layers and that for the upper mantle Birch's law which relates  $V_P$  and  $\rho$  applies.

If velocity and density models are constrained by observations one can also test how well the profiles agree with a homogeneous self-compressing (A-W) layer. The deviations from adiabatic self-compression can be expressed in terms of the Bullen or inhomogeneity parameter,  $\eta$ :

$$\eta = -\frac{\phi}{\rho g} \frac{d\rho}{dr} \quad (2.7)$$

For a homogenous self-compressing layer  $\eta$  is equal to 1. If  $\eta > 1$ , density increases faster than for adiabatic compression (e.g., in the transition zone), if  $\eta < 1$  density increases less fast (e.g., in the asthenosphere). Deviations from 1 can be due either to inhomogeneity, i.e., phase or chemical transitions, or to non-adiabaticity.

Once a density profile is established the gravitational acceleration and pressure can be calculated as a function of depth. Try this yourself for the PREM density model:

$$g(r) = \frac{Gm(r)}{r^2} = \frac{4\pi G}{r^2} \int_0^r \rho(r') r'^2 dr' \quad (2.8)$$

$$P(r) = \int_r^a \rho(r') g(r') dr' \quad (2.9)$$

The thus obtained  $g(r)$  hardly changes throughout the mantle, due to an approximate balance of the decreasing effect of the dense core as  $r$  increases, and the increasing effect of the added mantle mass with  $r$ .

## 2.6 Birch-Murnaghan equation of state

So we can measure seismic velocities in the interior of the Earth, and we have a reasonable picture of the 1-D density structure in the Earth as well, in other words, we have a good idea of the seismic properties of the mantle material at all depths. We can also measure in the laboratory the seismic properties of all candidates for 'pyrolite' under room pressure and temperature conditions. But if we want to compare those candidate properties to the measured properties of mantle materials, we need a means to extrapolate results from one to the other, in other words "compress" the laboratory data to mantle conditions, or "decompress" the seismic properties to room temperature and pressure. Therefore we need an 'equation of state' (EOS), which relates the density to pressure and temperature. This implies interpolation over many orders of magnitude in pressure difference over which the material deforms (compresses/decompresses) significantly. For such large deformation, linear stress-strain relationships are not valid anymore, which means that elastic properties are not easily extrapolated. So we need an EOS that is based on "finite strain theory". The most widely used one is the Birch Murnaghan EOS.

The strain tensor  $\epsilon_{ij}$  is generally defined as

$$ds^2 - ds_0^2 = 2\epsilon_{ij} dX_i dX_j \quad (2.10)$$

Under the assumption of small deformation we would be able to write this into the better known definition

$$\epsilon_{ij} = \frac{1}{2} \left( \frac{du_i}{dX_j} + \frac{du_j}{dX_i} \right) \quad (2.11)$$

but in our case this is not allowed. Instead, we assume isotropic deformation (i.e. when (de)compressing a material sample keeps its shape, but only changes volume):  $\epsilon_{ij} = \epsilon \delta_{ij}$ , with  $\delta_{ij}$  the Kronecker delta, which then gives:

$$ds^2 - ds_0^2 = 2\epsilon ds^2 \quad (2.12)$$

This again gives

$$ds = (1 - 2\varepsilon)^{-1/2} ds_0 \quad (2.13)$$

For a specific 3-D volume  $V_0 = ds_0 \times ds_0 \times ds_0$  this is:

$$V = (1 - 2\varepsilon)^{-3/2} V_0 \quad (2.14)$$

$$\rho = \frac{1}{V} = (1 - 2\varepsilon)^{3/2} \rho_0 \quad (2.15)$$

$$(2.16)$$

where  $\varepsilon$  is positive for dilation (extention) and negative for compression.  $f$  is defined as the opposite:  $f = -\varepsilon$ , and is positive with compression.

$$V = (1 + 2f)^{-3/2} V_0 \quad (2.17)$$

$$\rho = \frac{1}{V} = (1 + 2f)^{3/2} \rho_0 \quad (2.18)$$

$$(2.19)$$

During adiabatic (de)compression, deformation energy  $\Psi$  will lead to an increase in internal energy  $U$ :  $d\Psi = dU$ . Using the first thermodynamic law  $dU = TdS - pdV$  with  $dS = 0$  gives

$$p = \left[ -\frac{\partial U}{\partial V} \right]_S = \left[ -\frac{\partial \Psi}{\partial V} \right]_S \quad (2.20)$$

Now we write

$$\Psi = \Psi_0 + \Psi_1 f + \Psi_2 f^2 + \Psi_3 f^3 + \dots \quad (2.21)$$

For  $f = 0$ ,  $\Psi = 0$  as well, so  $\Psi_0 = 0$ . Both dilation and compression give a positive  $\Psi$ , so also  $\Psi_1 = 0$ . Ignoring fourth order terms then gives:

$$\Psi = \Psi_2 f^2 + \Psi_3 f^3 \quad (2.22)$$

With  $p = \left[ -\frac{\partial \Psi}{\partial V} \right]_S = \left[ -\frac{\partial \Psi}{\partial f} \right]_S \left[ -\frac{\partial f}{\partial V} \right]_S$  and Equations 2.14 and 2.22, we can write

$$p = \frac{1}{3V_0} (1 + 2f)^{5/2} (2\Psi_2 f + 3\Psi_3 f^2) \quad (2.23)$$

Using the definition of  $k_s$ :

$$k_s = \rho \left[ \frac{\partial p}{\partial \rho} \right]_S = \rho \left[ \frac{\partial p}{\partial f} \right]_S \left[ \frac{\partial f}{\partial \rho} \right]_S \quad (2.24)$$

with Equations 2.15 and 2.23, we find

$$k_0 = k_s(p = 0, f = 0) = \frac{2\Psi_2}{9V_0} \quad (2.25)$$

Defining  $\xi = \frac{-\Psi_3}{6V_0 k_0}$  leads to the Birch-Murnaghan EOS:

$$p = 3k_0 f (1 + 2f)^{5/2} (1 - 2\xi f) \quad (2.26)$$

Using Equation 2.24 for the incompressibility  $k_s$  and the definition of the seismic parameter  $\phi = k_s/\rho$ , similar expression for those (seismically measurable) quantities can be found. This allows for the decompression of seismic properties to room pressure. Extrapolation to room temperature is usually not done as laboratory experiments can be done in an oven under mantle temperatures.

## 2.7 Mantle phase transitions

The seismic velocities and density in the transition zone and lower mantle are reasonably explained by a constant composition which undergoes phase transitions as pressure increases. There is however some remaining misfit that fuels the debate whether phase transitions are the only effect. There are however also remaining uncertainties

in the seismic models, as well as in the mineral physics data and their extrapolation to high pressure and temperature. Discontinuities are studied seismically using reflected and converted waves. Discontinuities at various depths (between the Moho and 1200 km) have been proposed, but the only ones that are consistently and globally observed are those located approximately at 410 and 660 km depth. Several seismic observables help to constrain the exact character of the discontinuities:

- the depth and lateral variation in depth of the discontinuities
- the amplitude of the velocity and density jumps
- the sharpness of the seismic discontinuities

Depth is the best-constrained property of the discontinuities. The estimates for the "410" range from 390 to 430 km depth and for the "660" from 650 to 680 km depth. Several, mainly long-period, studies have also detected a discontinuity between 500 and 520 km depth. Uncertainties in the depths are mainly due to corrections that have to be applied for shallower mantle and crustal velocity structure. The discontinuity depths agree well with the laboratory predicted transitions from olivine ( $\alpha$ ) to wadsleyite ( $\beta$ -spinel), wadsleyite to ringwoodite ( $\gamma$ -spinel), and ringwoodite to perovskite+magnesiowüstite, thus favoring their interpretation as phase transitions. Garnet also transforms in the same depth ranges but over much broader intervals and is therefore thought to not contribute to the sharp seismic discontinuities. The interpretation of the discontinuities as phase transitions fixes their P,T condition thus giving one of the few points where absolute mantle temperature can be estimated.

Lateral variations in discontinuity depth potentially provide information on lateral variations in temperatures. The position of a single composition phase transition is described by the Clapeyron slope,  $\frac{dP}{dT}$ :

$$\frac{dP}{dT} = \frac{\Delta S}{\Delta V} \quad (2.27)$$

From thermodynamics and laboratory data it has been estimated that the olivine to  $\beta$ -spinel transition has a positive Clapeyron slope of 3-4 MPa/K. This would lead to its elevation in cold subducting slabs relative to the surrounding mantle. The same applies for the  $\beta$ -spinel to  $\gamma$ -spinel transition, which has a measured Clapeyron slope of around 5 MPa/K (but only a small jump of  $\sim 1\%$  in velocity and density). In contrast, the  $\gamma$ -spinel to perovskite transition has been found to have a negative Clapeyron slope of around -2 MPa/K, which would lead to its depression inside a cold slab relative to the surrounding mantle. Seismically, discontinuity topography of 20-40 km has been observed, which is consistent with 600-800 K thermal anomalies as expected in subduction zones. On average "660" shows larger topography than "410", which is just opposite of what is expected based on the experimental Clapeyron slopes. In some regions (often subduction zones) the topography on "410" and "660" is found to be negatively correlated as expected for a similar thermal anomaly and Clapeyron slopes with opposite signs. But in other regions such a correlation is not apparent. The estimates of lateral variations in discontinuity depth may be affected by Fresnel zones and the geometrical configuration of the data. Furthermore temperature variations at 410 and 660 may not be the same. The variations in phase transition depth can affect the dynamics of the flow. While a positive Clapeyron slope acts flow-enhancing, a negative Clapeyron slope results in local density anomalies that impede the flow. Seismic observations are most consistent with flow passing through "660". This is consistent with geodynamic models that include the effect of an endothermic phase transition with the experimental Clapeyron slope for the  $\gamma$ -spinel to perovskite transition. These models show that flow is slowed but not completely blocked by the phase transition.

Several phases that are used to study discontinuities are sensitive to impedance jump. In this way velocity and density jumps at the discontinuities have been estimated. The amplitude of the seismic velocity jumps at 410 and 660 km depth in the global 1-D models is larger than predicted for a pyrolite model. However, a wide range of velocity jumps (differing by up to a factor of 2) has been estimated in various studies. At least in part the spread in observations may be due to the different types of data used. Well-constrained velocity and density jumps would help to resolve whether any changes in composition occur at the discontinuities.

From reflected waves and triplications the width of the seismic discontinuities has been estimated to be about 5 km for the 410 and the 660 km discontinuity. Mineral physics data for olivine indicate a wider transition for olivine to  $\beta$ -spinel (8-19 km) than for  $\gamma$ -spinel to perovskite (1-4 km). Thus the transitions in olivine are predicted to be wider than observed seismically. But seismic imaging effects may make this transition look narrower and thus consistent with the mineral physics constraints. More problematic is the  $\beta$ -spinel to  $\gamma$ -spinel transition that is thought to occur over a 30-150 km depth range, which would make it seismically invisible. Variations in iron and water content can change the sharpness (as well as the depth) of the phase transition. A combination of phase transition observations may help to eventually determine whether any changes in composition occur.

## 2.8 3-D structure

Three-dimensional seismic structure (including lateral variations in depth of the discontinuities) can provide important constraints on the dynamics of the mantle. How well such variations can be imaged is discussed in the seismic tomography class. Largely, the lateral variations in seismic velocities are attributed to lateral variations in temperature, as expected in a thermally convecting system. But besides the discussion about possible variations in mantle chemistry with depth there is also an ongoing discussion about lateral variations in composition playing a role in mantle dynamics. What is clear is that the lithosphere is chemically differentiated, and these products are in part (in the case of oceanic lithosphere), recycled into the mantle. Whether oceanic crust and lithosphere are subsequently efficiently mixed again or remain as separate "blobs" in the mantle for any significant amount of time is unclear.

## 2.9 Additional reading on composition structure

[Davies(1999)] - Chapters 14.2 and 7.5

[Drake and Richter(2002)]

[McDonough and Sun(1995)]

[Ranalli(1995)] - Chapter 7.6

## 2.10 Additional reading on seismic structure

[Bullen and Bolt(1985)]

[Davies(1999)] - Chapter 5

[Duffy and Anderson(1989)]

[Dziewonski and Anderson(1981)]

[Jackson and Rigden(1998)]

[Ranalli(1995)] - Chapter 6

[Helffrich(2000)]

[Shearer(2000)]



# Bibliography

- [Bullen and Bolt(1985)] K. Bullen and B. Bolt. *An introduction to the theory of seismology*. Cambridge University Press, 1985.
- [Davies(1999)] G. F. Davies. *Dynamic Earth:Plates, Plumes and Mantle Convection*. Cambridge University Press, Cambridge, 1999.
- [Drake and Richter(2002)] M.J. Drake and K. Richter. Determining the composition of the Earth. *Nature*, 416: 39–44, 2002.
- [Duffy and Anderson(1989)] T.S. Duffy and D.L. Anderson. Seismic velocities in mantle materials and the mineralogy of the upper mantle. *Journal of Geophysical Research*, 94:1895–1912, 1989.
- [Dziewonski and Anderson(1981)] A.M. Dziewonski and D. L. Anderson. Preliminary reference earth model. *Physics of the Earth and Planetary Interiors*, 25:297–356, 1981.
- [Helffrich(2000)] G. R. Helffrich. Topography of the transition zone seismic discontinuities. *Review of Geophysics*, 38:141–158, 2000.
- [Jackson and Rigden(1998)] I. Jackson and S.M. Rigden. Composition and temperature of the earth’s mantle: seismological models interpreted through experimental studies of earth’s materials. In I. Jackson, editor, *The Earth’s Mantle: Composition, Structure and Evolution*. Cambridge University Press, Cambridge, 1998.
- [McDonough and Sun(1995)] W. F. McDonough and S.-s. Sun. The composition of the Earth. *Chemical Geology*, 120:223–253, 1995.
- [Ranalli(1995)] G. Ranalli. *Rheology of the earth*. Chapman and Hall, London, 2nd edition, 1995.
- [Shearer(2000)] P.M. Shearer. Upper mantle seismic discontinuities. In A. M. Forte, R. C. Liebermann, G. Masters, and L. Stixrude, editors, *Earth’s deep interior: Mineral physics and tomography from the atomic to the global scale*, pages 115–131. 2000.